AIMS Mathematics

http://www.aimspress.com/journal/Math

AIMS Mathematics, 5(5): 4229–4259.
DOI:10.3934/math.2020270
Received: 31 January 2020
Accepted: 19 March 2020
Published: 06 May 2020

*Review*

# Nonlinear dynamics of dewetting thin films

**Thomas P. Witelski***

Department of Mathematics, Duke University, Box 90320, Durham NC 27708-0320, USA

* **Correspondence:** Email: witelski@math.duke.edu; Tel: +19196602841.

**Abstract:** Fluid films spreading on hydrophobic solid surfaces exhibit complicated dynamics that describe transitions leading the films to break up into droplets. For viscous fluids coating hydrophobic solids this process is called "dewetting". These dynamics can be represented by a lubrication model consisting of a fourth-order nonlinear degenerate parabolic partial differential equation (PDE) for the evolution of the film height. Analysis of the PDE model and its regimes of dynamics have yielded rich and interesting research bringing together a wide array of different mathematical approaches. The early stages of dewetting involve stability analysis and pattern formation from small perturbations and self-similar dynamics for finite-time rupture from larger amplitude perturbations. The intermediate dynamics describes further instabilities yielding topological transitions in the solutions producing sets of slowly-evolving near-equilibrium droplets. The long-time behavior can be reduced to a finite-dimensional dynamical system for the evolution of the droplets as interacting quasi-steady localized structures. This system yields *coarsening*, the successive re-arrangement and merging of smaller drops into fewer larger drops. To describe macro-scale applications, mean-field models can be constructed for the evolution of the number of droplets and the distribution of droplet sizes. We present an overview of the mathematical challenges and open questions that arise from the stages of dewetting and how they relate to issues in multi-scale modeling and singularity formation that could be applied to other problems in PDEs and materials science.

**Keywords:** nonlinear parabolic partial differential equations; fluid dynamics; thin film equation; dewetting; finite-time singularities; long-time asymptotics
**Mathematics Subject Classification:** 76A20, 76D08, 76E17, 35K25, 35Q35

## 1. Introduction

Fluid dynamics is a long-standing source of challenging problems for mathematical analysis; one of these is describing the spreading of thin layers of viscous fluids on solid surfaces. Sometimes called "coating flows" [163, 185], these problems occur ubiquitously in nature (dew on leaves of plants [29,

57, 136] and tear films on the eye [31]) and in applications like painting of surfaces and lubrication of machine parts. Parallel to the long history of use of lubrication models in basic physics and engineering applications, the past few decades have seen the growth of mathematical interest in the nonlinear partial differential equations (PDE) that describe these systems. These problems can exhibit very rich forms of behaviors including finite-time singularities, self-similar solutions, free boundary problems, pattern-forming instabilities and long-time coarsening. This paper gives a brief overview of one class of these problems that includes these behaviors.

While second-order linear advection-diffusion models for transport in bulk flows of fluids have been well studied, there is a strong need to better understand the more complicated behaviors occurring in free-surface flows where surface tension and materials properties play important roles. Advances in engineering processes (for biological testing and other applications in microfluidics) allowing for more precise control of small quantities of fluids have sparked the need to explore these subtle influences. Avoiding loss of volume and contamination of tiny samples of fluids is another key concern in these processes. Fluid samples are more easily and reliably moved if their tendency to adhere to the solid substrate is reduced – achieving this has motivated a lot of work on the development of *hydrophobic* (water-repelling) materials making use of chemical properties of the materials or physical texturing of the surface (commonly used in synthetic fabrics and materials like teflon). Fluids placed on such repellent surfaces will undergo *dewetting*, which is manifested as a sequence of instabilities that progressively reduce the overall contact of the fluid with the solid [13, 57, 101, 106, 143, 172, 186–189].

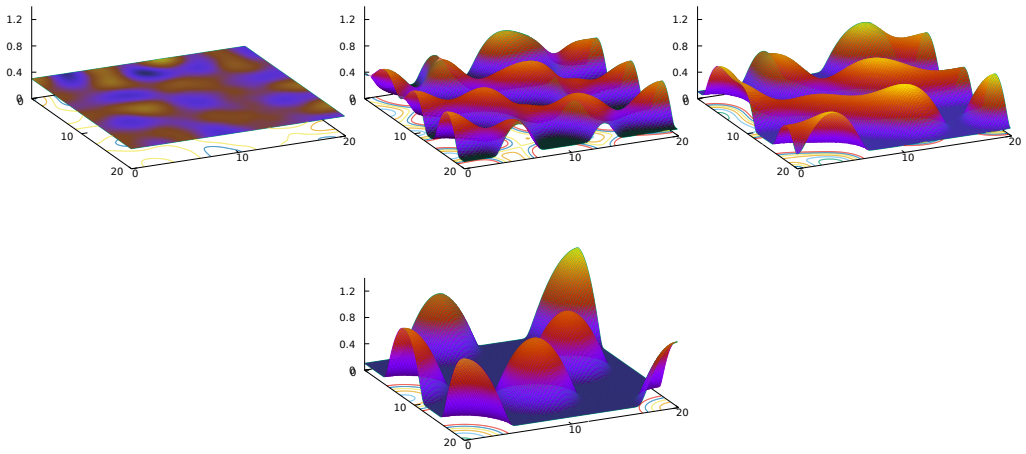


**Figure 1.** A sequence of time profiles from a numerical simulation of dewetting starting from small perturbations of a nearly-uniform layer, with spatial structure that grows in amplitude and then evolves to yield sets of droplets.

Mathematical modeling of dewetting behavior has produced a rich body of research showing that most of the essential features of the dynamics can be obtained from analysis and numerical simulations of partial differential equations of the general form

$$\frac{\partial h}{\partial t} = \nabla \cdot \left( h^3 \nabla \left[ \Pi(h) - \nabla^2 h \right] \right), \tag{1.1}$$

where $h(x, y, t)$ gives the evolving local height (thickness) of the fluid film and the *disjoining pressure* function $\Pi(h)$ characterizes the wetting properties of the solid surface relative to the fluid's tendency to spread under the influence of surface tension and other forces.

Following a brief sketch of the formulation of (1.1), we review the mathematical development of the various stages of the dewetting process spanning multiple length- and time-scales:

1. Short-time: initial linear instability and finite-time rupture
2. Intermediate: propagation of dewetting rims and instabilities of fluid ridges
3. Long-time: formation of quasi-steady droplets and multi-scale models of coarsening dynamics

and closing comments will address further directions for mathematical analysis.

## 2. Formulation of the model equation

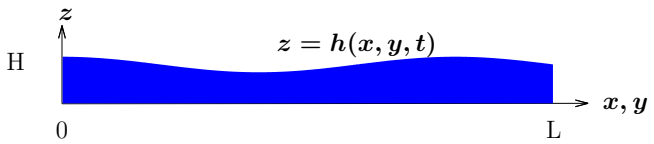


**Figure 2.** A schematic representation of the free-surface flow of a slender layer of a fluid of height $z = h$ on a flat solid surface, $z = 0$.

The mathematical formulation of classical lubrication models for thin film flows relies on two key assumptions – that the viscosity of the fluid is large, and that the fluid film is slender and slowly varying. These allow for the governing equations of fluid dynamics to be reduced down to a more tractable problem – a single nonlinear PDE as an evolution equation for the local height of the fluid layer.

The flow of incompressible Newtonian fluids is governed by the Navier-Stokes equations,

$$\mathrm{Re}\left(\frac{\partial \vec{\mathbf{u}}}{\partial t} + \vec{\mathbf{u}} \cdot \nabla \vec{\mathbf{u}}\right) = -\nabla p + \nabla^2 \vec{\mathbf{u}}, \qquad \nabla \cdot \vec{\mathbf{u}} = 0,$$

where $\vec{\mathbf{u}}$ is the fluid's velocity, $p$ the pressure field and the Reynolds number Re is a dimensionless parameter that describes the relative importance of inertial effects vs. viscous dissipation. For the slow motion of very viscous fluids, the "creeping flow" limit of $\mathrm{Re} \to 0$ reduces the equations to the Stokes equations [1, 128, 158],

$$\vec{\mathbf{0}} = -\nabla p + \nabla^2 \vec{\mathbf{u}}, \qquad \nabla \cdot \vec{\mathbf{u}} = 0.$$

While these governing equations are linear and time-invariant, the overall problem is nonlinear and time-dependent due to the boundary conditions that are imposed at the free surface of the fluid mass. In general, numerical methods are needed for these free boundary problems for Stokes flows [170, 173].

However, if the fluid occupies a long thin layer, namely a region with $0 \le (x, y) \le L$ and $0 \le [z = h(x, y, t)] < H$ then considering the aspect ratio, $\delta = H/L$, as a small parameter, a long-wave limit can be applied to obtain an asymptotic reduction for $\delta \to 0$, see Figure 2. The velocity can then be separated into components parallel and perpendicular to the solid boundary, $\vec{\mathbf{u}} = \vec{\mathbf{u}}_{\parallel} + u_{\perp}\hat{\mathbf{n}}$ and here $\hat{\mathbf{n}} = \hat{\mathbf{k}}$. For $\delta \to 0$, the leading order velocity is $\vec{\mathbf{u}} \sim \vec{\mathbf{u}}_{\parallel}$ and the quasistatic pressure is uniform across

the thickness of the film, $p \sim p(x, y, t)$. Applying boundary conditions on $u_\perp$ at the impermeable solid surface and free surface of the layer yields an equation for the conservation of the fluid mass of the form

$$\frac{\partial h}{\partial t} = \nabla \cdot (m(h)\nabla p)\,, \tag{2.1}$$

where $m(h)$ is a mobility coefficient and the mass flux is $\mathbf{J} = -m(h)\nabla p$. The form of the mobility depends on the boundary conditions for $\vec{\mathbf{u}}_\parallel$; the classic no-slip boundary condition [122] (zero tangential velocity at a fixed solid boundary) gives $m(h) = h^3$ yielding the classic Reynolds lubrication equation [4, 42, 147, 161],

$$\frac{\partial h}{\partial t} = \nabla \cdot \left(h^3 \nabla p\right). \tag{2.2}$$

Some forms for the mobility can be derived from models with slip effects at the solid surface, i.e. $m(h) = \beta h^2 + h^3$ corresponds to the Navier slip boundary condition [93]. For flows with stronger slip effects, or larger velocities, inertial effects can become important and different classes of models can be constructed involving coupled equations for $h$ and the mass flux [111, 145, 175]. In single-equation lubrication models, all physical effects considered are expressed by contributions to pressure functional, $p[h]$. In the simplest case, gravity-driven spreading is described by a hydrostatic pressure, $p = h$, yielding the classic porous medium equation [9, 210],

$$\frac{\partial h}{\partial t} = \nabla \cdot \left(h^3 \nabla h\right). \tag{2.3}$$

In problems involving global coupling of the film flow (with electric fields or thermodynamic effects) the pressure can be a nonlocal operator [67, 205].

If surface tension is the only effect considered, the pressure is proportional to the Gaussian curvature of the free surface $z = h(x, y, t)$. In the long wave limit, the leading order form is $p \sim -\nabla^2 h$; using this with $m(h) = h^n$ for $n \geq 0$ yields the *thin film equation* [17, 19, 30, 79–81, 113, 114, 147]

$$\frac{\partial h}{\partial t} = -\nabla \cdot \left(h^n \nabla [\nabla^2 h]\right). \tag{2.4}$$

This equation has been the focus of many rigorous analytical studies starting from the key paper of Bernis and Friedman in 1990 [16]. Physically meaningful solutions representing fluid film thicknesses must be non-negative, $h \geq 0$, but in contrast to (2.3), (2.4) does not have a maximum principle and consequently solutions starting from positive initial data may not remain positive for all times. Careful analysis showed that positivity is maintained for solutions if $n$ is large enough ($n \geq 3.5$) [16, 20]. Analysis of singularities in problems for (2.4) has been a source of continuing interest [23, 24, 41]. Further studies have addressed questions about the regularity, existence, uniqueness and speed of propagation of compactly supported weak solutions representing fluid droplets [15, 23, 24]. Existence of non-negative solutions was shown for $n \geq 1$ [16] and results on some properties have been obtained on ranges of $n$ (and might be restricted to one dimension) [26, 35, 48]. Additionally, physical arguments for spreading drops in the viscous, no-slip case, $n = 3$ in (2.4), showed that motion of the edge of support (also called the "contact line" or interface) would require unphysical singular forces [103].

Consequently, many approaches have been proposed for addressing these issues using PDE analysis [16, 22, 23, 38, 80, 81, 89], physical considerations [113, 191] and numerical methods for computing

solutions [95,225]. In [16] a positivity-preserving regularization of (2.4) was introduced by modifying the mobility function $m(h)$; this was also extended to numerical methods in [225]. Other papers have focused on removing the stress singularity at moving contact lines by incorporating slip in the mobility [145, 191].

A different physically-motivated approach regularizes solutions by modifying the pressure in (2.2) [29, 56]. Since (2.4) describes flows driven by surface tension effects only, it cannot distinguish differences due to material properties of the substrate, like water's tendency to spread on glass (a hydrophilic solid) vs. water's break-up into droplets on a hydrophobic surface like a teflon-coated frying pan. Such fluid-solid interactions can be characterized by calculating an effective potential for the averaged influence of molecular forces between the fluid and the solid [102, 105, 192]. For the simplest models, based on van der Waals interactions, this yields a potential depending only on the local fluid film thickness, $U(h)$. The derivative of $U$ with respect to changes in film height gives a contribution to the pressure called the *disjoining pressure*, $\Pi(h) = dU/dh$. Consequently, writing the total pressure as

$$p = \Pi(h) - \nabla^2 h, \tag{2.5}$$

we recover equation (1.1),

$$\frac{\partial h}{\partial t} = \nabla \cdot \left( h^3 \nabla \left[ \Pi(h) - \nabla^2 h \right] \right), \tag{2.6}$$

as a basic thin film model incorporating the influences of both surface tension and substrate wetting properties. The dynamics in this model, and (2.1) more generally, can be described in terms of a monotone decreasing energy functional,

$$E = \iint U(h) + \tfrac{1}{2}|\nabla h|^2 \, dA \qquad \text{with} \qquad \frac{dE}{dt} = -\iint m(h)|\nabla p|^2 \, dA \le 0. \tag{2.7}$$

The resulting gradient flow description from (2.7) has been used extensively in many analytical studies [39, 125] and formulation of extended models [199, 200]. Another important basic property of (2.6) is that the mass, $M = \iint h \, dA$, is conserved, which follows from the equation being in divergence form.

Typical forms of the disjoining pressure decay like $\Pi(h) = O(h^{-3}) \to 0$ as $h \to \infty$ [102]. This is consistent with the expectation that molecular effects should have negligible influences on the dynamics of thick films. The coefficient scaling the disjoining pressure is proportional to the Hamaker constant, which describes the strength of van der Waals molecular forces [192]. Disjoining pressures $\Pi(h) \sim A/h^3$ with $A > 0$ describe disjoining forces for the hydrophobic interactions while $A < 0$ represents conjoining forces in the hydrophilic case. These two cases correspond to whether the second order operator in (2.6), $\nabla \cdot (h^3 \nabla[\Pi(h)])$, is destabilizing or diffusive respectively.

## 3. Early-stage dynamics

For fluids starting as nearly uniform layers describing the early-time dynamics of fluid coating layers on hydrophobic surfaces can be accomplished from the most basic representation of the van der Waals disjoining pressure, $\Pi(h) = 1/(3h^3)$ [179,211]. In one spatial dimension this yields the evolution equation

$$\frac{\partial h}{\partial t} = -\frac{\partial}{\partial x}\left( \frac{1}{h}\frac{\partial h}{\partial x} + h^3 \frac{\partial^3 h}{\partial x^3} \right), \tag{3.1}$$

as studied in [217] and many later papers [112, 224]. We will go on to describe the richer behaviors that occur in two dimensions in later sections.

On a finite domain with length $L$, with Neumann no-flux boundary conditions, uniform layers of constant thickness, $h = \bar{h}$, are equilibrium solutions for any $\bar{h} > 0$. Linear stability analysis with respect to infinitesimal perturbations,

$$h(x,t) \sim \bar{h} + \delta \cos(k\pi x/L) e^{\lambda_k t} \qquad \text{for } \delta \to 0 \tag{3.2}$$

yields

$$\lambda_k = \frac{k^2\pi^2}{L^2}\left(\frac{1}{\bar{h}} - \frac{k^2\pi^2}{L^2}\bar{h}^3\right) \qquad k = 0, 1, 2, \cdots \tag{3.3}$$

and shows that the second order term has a destabilizing influence. Further, there is a critical thickness, $\bar{h}_c = \sqrt{L/\pi}$, below which the uniform film is unstable [220],

$$\begin{cases} \bar{h} < \bar{h}_c: & \text{Thin films are unstable,} \\ \bar{h} > \bar{h}_c: & \text{Thick films are linearly stable to infinitesimal perturbations.} \end{cases}$$

More comprehensive studies of the steady states of a class of fourth-order parabolic PDEs including (3.1) were done in [110, 123–126] and further analysis of the dynamics in [23, 24, 49]. Applying bifurcation theory at the critical thickness $\bar{h}_c$ shows it to be a subcritical pitchfork bifurcation point [220] with another branch of equilibria having non-trivial spatial structure existing for average thickness $\bar{h} \geq \bar{h}_c$. These spatially periodic solutions can be shown to be unstable and they act as a separatrix between two stable regimes of dynamics, either: (i) relaxation to the uniform thick film, or (ii) film rupture, where the minimum thickness vanishes in finite-time at some point $x_c$ (see Figure 3),

$$h(x_c, t) \to 0 \qquad \text{as} \quad t \to t_c, \tag{3.4}$$

which yields a singularity of the disjoining pressure term.

### *3.1. Finite-time rupture singularities*

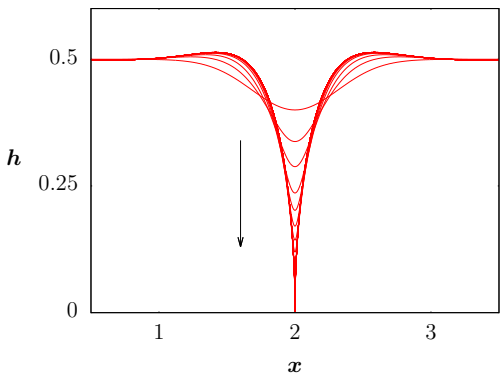


**Figure 3.** Finite-time rupture being approached in time profiles from a numerical solution of (3.1) starting from a small perturbation of an unstable flat film.

Dimensional analysis of (3.1) shows that it is scale-invariant with respect to solutions of the form

$$h = O(\tau^{1/5}) \to 0, \qquad x = O(\tau^{2/5}) \to 0, \tag{3.5}$$

where $\tau = t_c - t \to 0$ is the time to the rupture (sometimes called a pinch-off [40] or touchdown [28,90] singularity). A consequence of this is that the problem can have a first-kind similarity solution [11,12] of the form

$$h(x,t) = \tau^{1/5} H(\eta), \qquad \eta = (x - x_c)/\tau^{2/5}; \tag{3.6}$$

such similarity solutions reaching singular behaviors at finite critical times are also called backward self-similar solutions [82]. Solution (3.6) can also be called a focusing solution since its spatial scale shrinks as the singularity is approached.

Zhang and Lister [224] showed that the rupture singularity of (3.1) is approached through a first-kind self-similar solution of the form (3.6). The similarity profile $H(\eta)$ satisfies a boundary value problem for the nonlinear ordinary differential equation (ODE),

$$-\tfrac{1}{5}\left(H - 2\eta\frac{dH}{d\eta}\right) = -\frac{d}{d\eta}\left(\frac{1}{H}\frac{dH}{d\eta}\right) - \frac{d}{d\eta}\left(H^3\frac{d^3H}{d\eta^3}\right) \qquad H(|\eta| \to \infty) \sim C|\eta|^{1/2}. \tag{3.7}$$

The far-field boundary condition follows from the localized nature of the singularity; namely, as the critical time is approached, while the singularity is approached at $x_c$, the evolution of the solution at finite distances away from $x_c$ continues smoothly, $h_t = O(1)$ for $|x - x_c| = O(1)$ as $t \to t_c$ [219,220].

Solving (3.7) numerically, it was found that an infinite sequence of distinct solutions, $H = H_j(\eta)$ with $j = 1, 2, 3, \cdots$, exist with different values for the far-field constant $C = C_j$, $C_1 > C_2 > C_3 > \cdots$ with $C_j \to 0$ as $j \to \infty$ [219,220,224]. Analytical support for these results was obtained by rescaling the problem as $H(\eta) = \epsilon^{2/5}\phi(z)$ with $\eta = \epsilon^{-1/5}z$ and $\epsilon = C^2 \to 0$ to yield the singular perturbation problem,

$$\tfrac{1}{5}\left(\phi - 2z\frac{d\phi}{dz}\right) - \frac{d}{dz}\left(\frac{1}{\phi}\frac{d\phi}{dz}\right) = \epsilon^2\frac{d}{dz}\left(\phi^3\frac{d^3\phi}{dz^3}\right) \qquad \phi(|z| \to \infty) \sim z^{1/2}. \tag{3.8}$$

Exponential asymptotics was used to consider Stokes phenomenon for the solutions analytically continued in the complex plane and determine a selection mechanism for the discrete $\epsilon_j = C_j^2$ values [37]. Further studies of self-similar rupture in related models have been recently considered in [50,51].

From all of the solutions of (3.7), linear stability analysis showed that only the first ($j = 1$) is stable to one-dimensional perturbations [220]. This is consistent with it being the only behavior leading to rupture observed in numerical simulations of (3.1). In the context of the full two-dimensional problem,

$$\frac{\partial h}{\partial t} = -\nabla\cdot(h^{-1}\nabla h + h^3\nabla[\nabla^2 h]), \tag{3.9}$$

one-dimensional solutions, $h = h(x,t)$, represent uniform rupture along lines. Analysis of the stable one-dimensional solution showed it to be linearly unstable to transverse two-dimensional perturbations [220]. Further work showed that only the $j = 1$ axisymmetric self-similar solution, $h = \tau^{1/5}H_1(r/\tau^{2/5})$, is linearly stable, corresponding to locally axisymmetric rupture at isolated points [219, 220]. This behavior is consistent with experimental observations in early-stage dynamics of dewetting films [131, 189].

The occurrence of singularities in models of fluid dynamics has been studied in many contexts as signs of dramatic transitions such as changes in topology [64–66]. Some aspects of the dynamics at the singularity may be unphysical (e.g. infinite forces, sub-atomic lengthscales) indicating that assumptions used to justify the governing equations have broken down and should be replaced by a more comprehensive model. Still, the simpler models make very valuable contributions by capturing the qualitative dynamics leading up to the singularity in a simple form (often as a self-similar solution).

A fundamental limitation of (3.1) is that its solutions cannot be continued to times after rupture occurs due to the singularity of the disjoining pressure term for $h \to 0$ [39]. To move forward in describing the rest of the dynamics of dewetting, we will see that it can be sufficient to keep (2.6) but to consider a revised form for the disjoining pressure.

### *3.2. The revised dewetting thin film model*

Finite-time rupture can be prevented by retaining higher-order terms in the expansion of the disjoining pressure. The balance of leading order disjoining forces with secondary conjoining forces (or "Born repulsion" [160]) can set a scale for molecular thin films (also called precursor or wetting layers) that are strongly adsorbed to the substrate, we will write this as $h = O(\epsilon) \ll 1$. A simple example of such a disjoining pressure is [85, 87, 88] (see Figure 4)

$$\Pi(h) = \frac{\epsilon^2}{h^3}\left(1 - \frac{\epsilon}{h}\right). \tag{3.10}$$

This and similar forms have been used in many physics and engineering studies of thin films [159–161, 183, 184]. In [21] it was shown that for a family of $\Pi(h)$ functions [96] including (3.10), solutions of (2.6) starting from positive initial data remain smooth and positive for all times. The resulting positive lower bound, $h \geq O(\epsilon)$, eliminates the possibility of rupture singularities and removes the trouble with moving contact lines for any $\epsilon > 0$. Consequently, (2.6) with $\Pi$ given by (3.10) is a physically motivated regularization of (3.1) that allows us to study all stages of dewetting.

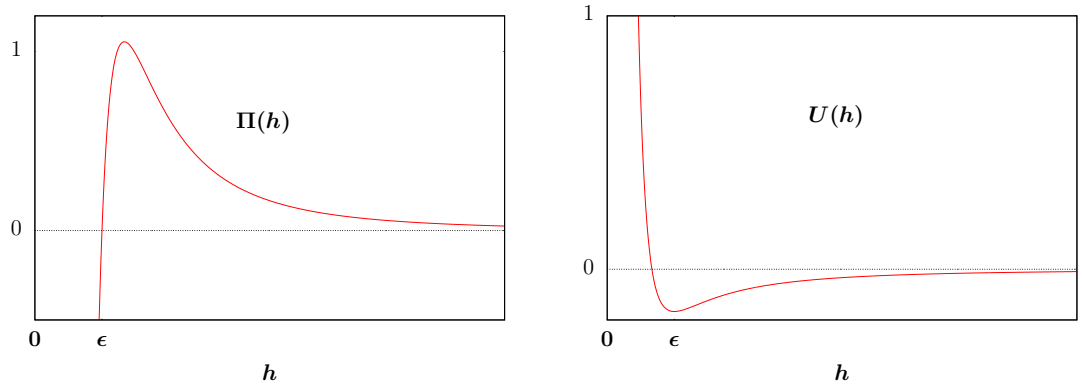


**Figure 4.** Plot of the regularized disjoining pressure $\Pi(h)$ (left), (3.10), and the corresponding potential energy $U(h)$ (right), (3.13).

Noting that (3.10) is a non-monotone function, (2.6) can be compared with Cahn-Hilliard models for the dynamics of binary phase separation in materials science [68, 104, 123, 139, 156, 181, 182]

$$\frac{\partial u}{\partial t} = \nabla \cdot \left(m(u)\nabla\left[f(u) - \nabla^2 u\right]\right), \tag{3.11}$$

where $u(x,t)$ is a conserved order parameter and $f$ is the derivative of a potential energy, $f(u) = F'(u)$. Mitlin [141] was one of the first researchers to draw attention to the connections between these models (with $h$ being analogous to $u$ and $\Pi(h)$ corresponding to $f(u)$), which have been used extensively in later studies [69,104,123,169,204]. For one example, generalizing the linear stability results (3.2, 3.3) for general mobilities and disjoining pressures yields

$$\lambda_k = -\frac{k^2\pi^2}{L^2} m(\bar{h}) \left( \Pi'(\bar{h}) + \frac{k^2\pi^2}{L^2} \right). \tag{3.12}$$

This form shows that thin homogeneous films with $\bar{h} < h_{\text{peak}}$ (where $\Pi'(h_{\text{peak}}) = 0$) will be stable while there will be an unstable range for films with negative $\Pi'(\bar{h})$. For Cahn-Hilliard models, the growth of instabilities from small-amplitude perturbations to unstable uniform states is called *spinodal decomposition* [91]; the analogous situation for unstable thin films has been called *spinodal dewetting* [27,167,169,190,208]

However, there are also some notable differences. For the Cahn-Hilliard equation, the potential energy $F(u)$ is a double-well function that determines two finite values for the stable homogeneous states from a common-tangent construction [157]. Between those two states is a finite unstable range of $u$ where $f'(u)$ is negative. Phase separation for (3.11) consists of the solution approaching one of the two stable homogeneous states everywhere except for narrow transition regions between those states. In contrast, for (3.10), the potential energy

$$U(h) = -\frac{\epsilon^2}{2h^2} + \frac{\epsilon^3}{3h^3}, \tag{3.13}$$

has only a single minimum and has $\Pi'(\bar{h}) < 0$ for all $\bar{h}$ in $h_{\text{peak}} < \bar{h} < \infty$ where $h_{\text{peak}} = 4\epsilon/3$ (see Figure 4). We will see that a consequence of this degenerate single-well form is that for (2.6), phase separation consists of the solution everywhere approaching either a nearly uniform precursor layer, $h = O(\epsilon)$, or one of a continuous family of near-equilibrium fluid droplet solutions. This behavior will be described in more detail in the later section on the long-time dynamics of dewetting.

## 4. Intermediate-time dynamics

The intermediate dynamics in dewetting extend the short-time local dynamics to give rise to patterned solutions depending on larger scales up to the size of the problem domain. We begin by giving a more complete description of the dynamics for the regularized model (2.6, 3.10) under conditions where the un-regularized model (3.9) would yield finite-time rupture. To build intuition we will examine behavior in the one-dimensional problem,

$$\frac{\partial h}{\partial t} = \frac{\partial}{\partial x}\left( h^3 \frac{\partial}{\partial x}\left[ \Pi(h) - \frac{\partial^2 h}{\partial x^2} \right] \right) \qquad \text{with} \qquad \Pi(h) = \frac{\epsilon^2}{h^3}\left(1 - \frac{\epsilon}{h}\right), \tag{4.1}$$

before describing the richer geometric structures occurring in the two-dimensional problem.

Starting from a perturbed nearly-uniform unstable layer with mean thickness $\bar{h} = O(1)$ the leading order evolution of (4.1) will follow the rupture dynamics described in section 3.1 during the times when $h \gg \epsilon$ everywhere since the disjoining pressure will be dominated by the destabilizing leading order term, $\Pi \sim \epsilon^2/h^3$, see Figure 5a. Because of the lower bound for solutions of (4.1), the singularity

will not be achieved and the "near-rupture" self-similar dynamics will proceed only until reaching $h_{\min} = O(\epsilon)$ [21]. After that, the minimum thickness remains bounded and the region where $h = O(\epsilon)$ expands to form a "hole" or "dry spot" [2, 27, 78, 140, 148, 149, 161, 190, 209]. These terms are very widely used and are appropriately suggestive of the structure of the solution but should not be taken to mean that the solution is literally changing topology or its region of support. The apparent "hole" is based on the distinct separation in scales between the nearly-uniform $O(\epsilon)$ precursor relative to the $h = O(1)$ film and the well-defined boundary between phases given by the effective contact line (made possible by the near-degeneracy of the mobility $m(h)$ for $h \ll 1$), see Figure 5. As assured by the results from [21], the entire substrate surface remains wetted with fluid ($h > 0$) and the solution is smooth everywhere for all $t \geq 0$ as the process of phase separation progresses to form the precursor and droplets.

The fluid displaced from the dry spots collects into growing "rims" or "ridges" that propagate into the surrounding film layer as the hole grows [189], see Figure 5b. The structure and dynamics of these dewetting rims approach an asymptotically self-similar form for long times when their growing heights become much larger than the $h = O(1)$ surrounding film [71, 144], see Figure 5c. The analysis involves several intermediate timescales and the motion of the rims is sensitive to slip effects [71, 72]. Whether the advancing face of the rims has monotone or oscillatory decay as it matches to the uniform surrounding film has been shown to relate to slip in the mobility function $m(h)$ and compares well against experimental studies of growing dry spots in the dewetting of polymer films [71, 73, 144, 145].

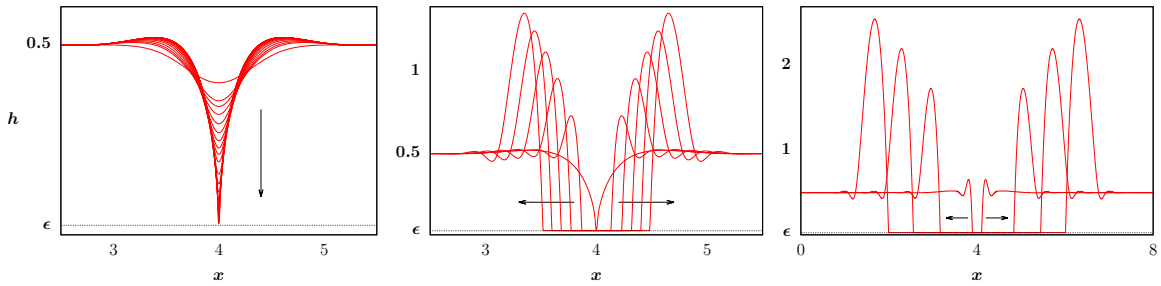


**Figure 5.** The intermediate-time dynamics of (4.1): (a) regularized near-rupture, (b) growth of a "dry-spot" and formation of dewetting "rims", (c) further growth of the hole and propagation of the rims.

The dry spots and the rims continue to grow as long as there is a surrounding film to expand into. In problems on larger domains where several holes have developed from rupture dynamics at different locations, the rims of adjacent holes will eventually run into each other, see Figure 6a. In one dimension, the colliding rims will merge to form a quasi-steady droplet, which will be the fundamental starting point for the long-time dynamics to be described in Section 5, see Figure 6b.

In the context of the rupture of two-dimensional films at isolated points, the profiles shown in Figure 5 can be understood to qualitatively correspond to one-dimensional cross-sections through an axisymmetric solution. Whether growing circular dry spots are stable to non-axisymmetric perturbations is a very important question for understanding the further stages of dewetting. Linear stability analysis of the dewetting rims to transverse perturbations (potentially leading to fingering or other pattern forming phenomena) is a challenging problem because the uniform rim is a time-dependent base state with growing lengthscales and hence traditional approaches for linear

stability analysis can only provide short-time estimates [115] and examinations of transient growth is needed [62, 116]. Recent numerical studies have demonstrated that careful choices for the form of the mobility $m(h)$ to properly represent slip effects on different materials will change the stability of moving rims, causing them to shed secondary droplets, in good agreement with experimentally observed behaviors [166].

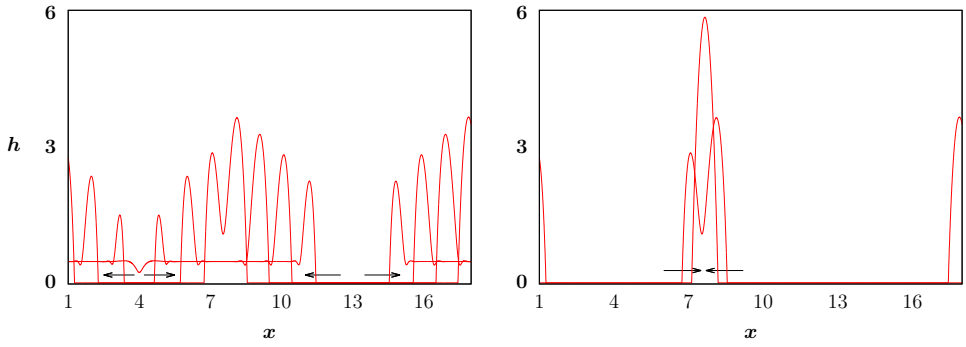


**Figure 6.** Later stages of intermediate dynamics in one dimension: (a) counter-propagation of dewetting rims from adjacent dry spots, and (b) eventual collision and merging of rims yielding the formation of a quasi-steady fluid droplet/ridge.

In two dimensions, colliding dewetting rims will form a nearly-stationary polygonal network of fluid ridges. Locally the ridges are nearly cylindrical with cross-sections being quasi-steady solutions of the one-dimensional problem (4.1), $h(x, y) \sim h(x)$. On a larger scale, the network structure can resemble a Voronoi diagram having cells centered at the well-separated original rupture points. Subsequently, each of the ridge segments can undergo a Rayleigh-type "pearling" instability and break-up into linear arrays of drops [59, 60]. Consequently, there would be lines of drops along the former positions of the ridges and large regions with no drops in the polygonal dry spots. This form of dynamics, based on stable growth of dry spots and break-up into droplets only after a network has formed, has been observed in experimental studies under appropriate conditions [106, 130, 166]. However there are also other scenarios for the intermediate dynamics that yield significantly different arrangements of droplets and have been approached using different modes of analysis. When the propagating dewetting rims are unstable, they can yield a more spatially uniform distribution of drops that were shed before the ridge network gets formed. At the other extreme, in [13] it was observed in experiments and numerical models that instabilities could generate a cascade of satellite dry spots forming in fractal-like patterns.

The scenarios outlined above involve localized perturbations initiating rupture at isolated locations followed by propagating instabilities determining the larger spatial patterns; these are generally called *nucleation-dominated dewetting* [100, 112]. A numerical simulation of this type of dynamics in a small domain is shown in Figure 7. The influence of the original rupture position can be seen to persist for significant lengths of time, see Figure 7bc.

In contrast, a different form of dynamics occurs for perturbation amplitudes growing uniformly across the entire domain. Figure 1 shows an example of such evolution, starting from small-amplitude random perturbations to a spatially uniform film. The early stages of the pattern-forming evolution of these solutions closely follow the predictions of linear stability analysis (3.12). In particular, in homogeneous dewetting rupture is reached at roughly the same time in the whole domain rather than spreading from isolated nucleations points. This mode of dynamics is called spatially homogeneous

instability or *spinodal dewetting*.

Thiele and collaborators [169, 204] and others [27, 142, 149, 188] have carefully considered nucleation vs. spinodal dewetting, making use of connections to stability analysis for Cahn-Hilliard models. The dramatically different dynamics shown in Figures 1 and 7 are directly tied to their initial conditions as both simulations were done on the same domain and with the same parameters in (2.6). While for short times they exhibit significantly different transients, for longer times they both might be thought to reach comparable states composed of droplets and precursor layers when phase separation is achieved (see final plots in each Figure). However, a close examination of these solutions show that they retain important differences – spinodal dewetting solutions have droplets that are closer to being uniform in size and spatial spacing, in contrast, nucleation creates drops with wider distributions of droplet sizes and spacings. These resulting arrays of near-equilibrium droplets form the initial conditions for the next stage of dynamics.

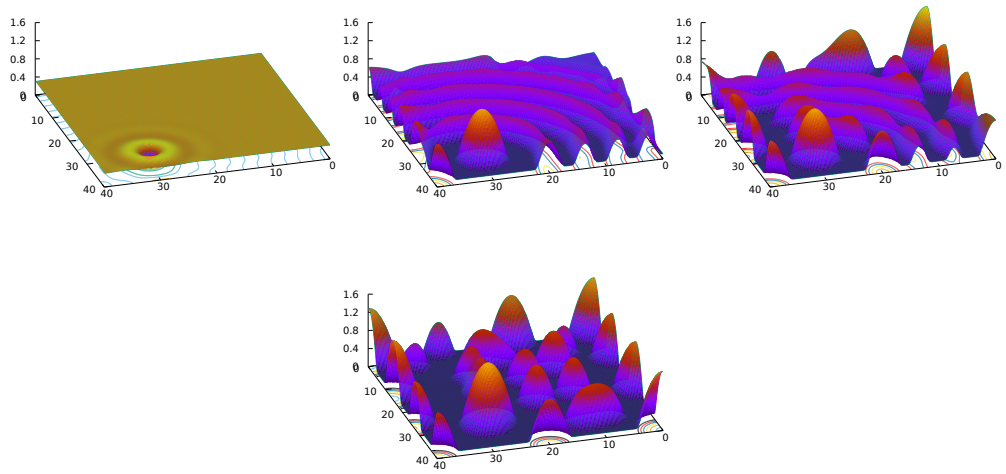

**Figure 7.** A sequence of time profiles from a numerical simulation of dewetting starting from a localized perturbation leading to near-rupture at a point, whose influence then propagates to the rest of the domain and eventually breaks up to form a set of droplets.

## 5. Long-time dynamics

In the aftermath of the dramatic changes in film structure and spatial transport of fluid mass produced by the intermediate dynamics, the fluid layer has been phase-separated into isolated fluid droplets and the nearly-uniform precursor, $h = O(\epsilon)$, between them. The subsequent dynamics will occur over long timescales since locally, each of the remaining droplets is close to being a steady state. However, globally the system is far from equilibrium [43] since any arrangement of non-identical droplets will lead to local mass fluxes. Moreover, since even spatial periodic arrangements of identical droplets are unstable equilibria [123], evolution from generic initial conditions must proceed further until a final stable equilibrium (a single droplet) is achieved. This gives rise to *coarsening dynamics*. We will present an overview of this regime of dynamics in terms of the one-dimensional model (4.1) following [87, 88] before describing the extension to two

dimensions [86].

Equilibrium solutions, $h = H(x)$, of (4.1) occur when the pressure is a uniform constant. In one-dimension, this yields a second-order ordinary differential equation for $H(x)$ parametrized by $\bar{p}$,

$$\frac{d^2H}{dx^2} = \Pi(H) - \bar{p}. \tag{5.1}$$

For each value of $\bar{p}$ in $0 < \bar{p} < \Pi(h_{\text{peak}})$, this equation has a homoclinic solution that approaches a far-field constant precursor height $H \to h_* \equiv \epsilon + O(\epsilon^2\bar{p})$ as $|x| \to \infty$. A simplified representation of the structure of this solution can be obtained by using matched asymptotics in the limit of $\epsilon \to 0$ [21, 87]. The droplet has a finite core region with $|h| \gg \epsilon$ where the pressure sets the constant curvature of the surface,

$$H(x;\bar{p}) \sim \tfrac{1}{2}\bar{p}(\bar{w}^2 - x^2) \qquad -\bar{w} < x < \bar{w} \tag{5.2}$$

where the droplet width can be shown to be inversely related to pressure and scaled by the potential to satisfy matching conditions to the surrounding thin film, $\bar{w}(\bar{p}) \sim \sqrt{2|U(\epsilon)|}/\bar{p}$. Consequently, the mass of the droplet is inversely proportional to the square of the pressure,

$$\bar{M}(\bar{p}) \sim \int_{-\bar{w}}^{\bar{w}} H\,dx \sim \frac{2^{5/2}}{3}|U(\epsilon)|^{3/2}\frac{1}{\bar{p}^2} \qquad \text{for } \bar{p} \to 0. \tag{5.3}$$

These droplet solutions can now be employed to reduce the evolution of the PDE to finite-dimensional dynamical system for the degrees of freedom associated with the drops.

Noting the existence of the continuous family of drops for any $\bar{M} > 0$ and the translational invariance of (4.1), every steady drop can be characterized by specifying its position $X$ and its pressure $P$. Quasi-steady evolution of an individual droplet can be examined by allowing these parameters to be slowly evolving functions of time on some timescale, $\tau = \sigma t$ with $\sigma \ll 1$, with comparable small perturbations to the solution,

$$h(x,t) = H(x - X(\tau); P(\tau)) + \sigma h_1(x,\tau) + O(\sigma^2). \tag{5.4}$$

The slow evolution can be expected to be driven by comparably small mass fluxes imposed on the droplet through the surrounding thin film, say due to the presence of other nearby drops [87]

$$J(-\ell) = \sigma\tilde{J}_-, \qquad J(\ell) = \sigma\tilde{J}_+. \tag{5.5}$$

At leading order in $\sigma$, the quasi-steady droplet solution satisfies (4.1) identically; at $O(\sigma)$ we obtain

$$-\frac{\partial H}{\partial x}\frac{dX}{d\tau} + \frac{\partial H}{\partial \bar{p}}\frac{dP}{d\tau} = \mathcal{L}h_1 \tag{5.6}$$

where $\mathcal{L}$ is the spatial operator for (4.1) linearized about $H(x - X; P)$ [87],

$$\mathcal{L}\phi \equiv \frac{\partial}{\partial x}\left(H^3\frac{\partial}{\partial x}\left[\Pi'(H)\phi - \frac{\partial^2\phi}{\partial x^2}\right]\right). \tag{5.7}$$

This is a non-self-adjoint singular operator with a two-dimensional nullspace corresponding to the two degrees of freedom in the leading order solution. To ensure the existence of solutions for $h_1$,

the Fredholm alternative must be applied to project (5.6) onto each of the adjoint nullfunctions. The resulting solvability conditions yield two evolution equations for the droplet's position and pressure in terms of the boundary fluxes,

$$\frac{dP}{dt} = C_P(P)(J_+ - J_-), \qquad \frac{dX}{dt} = -C_X(P)(J_+ + J_-), \tag{5.8}$$

where the coefficient functions are given in terms of integrals of $H(x)$ and can be reduced to functions of the droplet's pressure alone [87, 88]. Note that the artificial small parameter $\sigma$ scales out of (5.8) exactly and the dependence on the assumed domain size has a negligible influence.

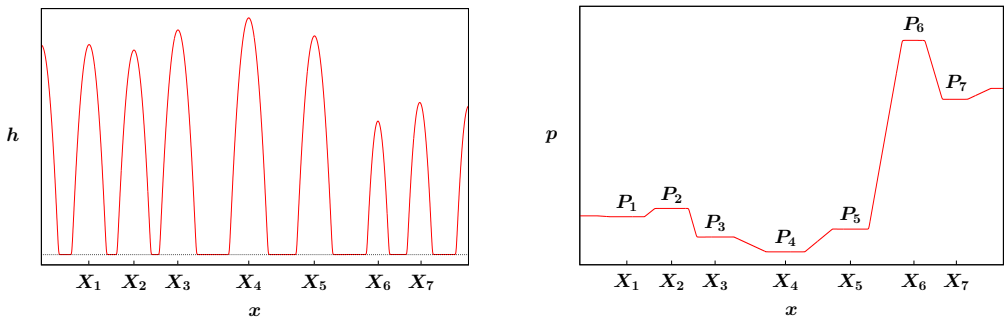


**Figure 8.** (a) The height profile $h(x, t)$ at a given time from (4.1) showing an array of seven drops at positions $X_n$, $n = 1, 2, \cdots, 7$, and (b) the corresponding pressure field $p(x, t)$ from (2.5) showing locally near-constant values of the pressure, $P_n$, in the core of each quasi-steady droplet.

It may seem tempting to use (5.3) to re-write (5.8) in terms of the more-intuitive mass of the droplet core. However while the droplet mass is only well-defined in the droplet cores, the pressure field is defined everywhere by (2.5) and is essential for closing the model by providing a relation between the pressures and the flux for interacting adjacent droplets. Figure 8 shows the height profile and pressure field at a given time from a numerical solution of (4.1) consisting of a typical array of droplets produced by dewetting. The drops vary in sizes but all have the characteristic parabolic core profile given by (5.2). Within the region of support of each drop ($X_n - \bar{w}(P_n) < x < X_n + \bar{w}(P_n)$) the pressure is nearly constant, $p(x) \approx P_n$, consistent with (5.1). The pressure is continuous everywhere and its value in the molecular thin film between the droplets matches the values $P_n$ at the drops. Under the assumptions that the molecular film is quasi-steady and nearly flat, Eq (4.1) can be reduced to an elliptic problem on the region between drops,

$$0 = \frac{\partial}{\partial x}\left(h^3 \frac{\partial}{\partial x}\left[\Pi(h)\right]\right), \tag{5.9}$$

which can be re-written as Laplace's equation applied to a new potential function,

$$0 = \frac{\partial^2}{\partial x^2}\left(V(h)\right) \qquad V(h) \equiv \int h^3 \Pi'(h)\, dh. \tag{5.10}$$

This potential then has a linear profile between drops, $V = Ax + B$, that is determined by Dirichlet boundary conditions to match the pressures/heights at the edges of the neighboring droplets. Then the

flux through the thin film is a constant, $J = -h^3\partial_x p = -\partial_x V$, and can be expressed in terms of the properties of the adjacent drops as

$$J_{n,n+1} = -\frac{V(h_*(P_{n+1})) - V(h_*(P_n))}{[X_{n+1} - \bar{w}(P_{n+1})] - [X_n + \bar{w}(P_n)]}. \tag{5.11a}$$

This relation for the flux combined with (5.8) yields a closed model for the evolution of the positions and pressures for a set of $N$ interacting droplets, $n = 1, 2, \cdots, N$,

$$\frac{dP_n}{dt} = C_P(P_n)(J_{n,n+1} - J_{n-1,n}), \qquad \frac{dX_n}{dt} = -C_X(P_n)(J_{n,n+1} + J_{n-1,n}). \tag{5.11b}$$

The heuristic argument from [87, 88] reviewed above has been also been examined using rigorous analysis based on a center manifold reduction [117, 118].

Numerical simulations [87, 88] show that the reduced ODE model (5.11ab) accurately predicts the evolution of the droplets in the PDE (4.1) while the solutions of the ODEs remain bounded and slowly varying. However the ODEs can generate finite-time singularities. These behaviors are not a spurious effect of simplifications used in the derivation but directly correspond to crucial behaviors in the PDE when the assumption of quasi-steady evolution are briefly violated.

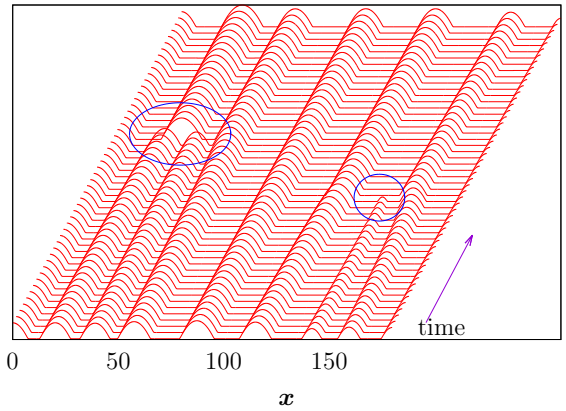


**Figure 9.** A numerical solution of the PDE (4.1) showing the slow evolution of the array of quasi-steady droplets shown Figure 8 punctuated by collapse and collision coarsening events.

Figure 9 shows a numerical simulation of (4.1) starting from the initial state composed of seven droplets shown in Figure 8. Over long ranges of time, the drops are seen to evolve smoothly, but the figure also highlights two types of events that would produce singular behavior in (5.11):

(a) Collapse: disappearance of an individual droplet due to its mass vanishing, $M_n \to 0$, corresponding to a finite-time singularity in its pressure, $P_n \to \infty$.
(b) Collision: merging of two adjacent drops when their regions of support overlap.

In both of these cases, the flux (5.11a) becomes singular; for collision because the denominator vanishes with the numerator remaining finite, and for collapse with the numerator diverging since $V(P \to \infty) \to \infty$ while the denominator remains finite. Further, in both cases, after the time of the singular event ($t_c$), the solution will contain one drop less, i.e. $N \to N - 1$; these are *coarsening events* for this problem.

The implications of coarsening for the ODE system (5.11) are that the dynamical system must be understood to be defined piecewise in time. Namely, ODEs (5.11b) can be integrated in time from appropriate initial conditions until a singularity occurs at $t \to t_c^-$. At that time, when PDE (4.1) would be briefly exhibiting rapid far-from equilibrium dynamics, the ODEs must be replaced by a different relation to map from the quasi-steady state of the droplets before $t_c$ to a new post-coarsening quasi-steady state for $t > t_c^+$ from which the ODEs can be resumed. Sometimes called a *coarsening rule*, this would reduce the order of the ODE system, $N \to N - 1$, and re-assigning drop-adjacency after removing the collapsed droplet or merging the masses of the collided droplets at a new effect droplet position. Models combining smooth evolution generated by differential equations with maps that are applied at discrete times to represent singular events are generally called *hybrid dynamical systems* and have been used in modeling problems like mechanical systems with impacts [58]. In the context of coarsening in a Cahn-Hilliard problem, this type of model has been called a *coarsening dynamical system* [214], and similar models have been used in other physical systems having interacting localized structures [97].

The extension of these dynamics to the full problem for a set of droplets on a two-dimensional surface builds in a natural way from the model described above. The individual droplet states will now be solutions of the semilinear elliptic PDE,

$$\nabla^2 H = \Pi(H) - \bar{p}. \tag{5.12}$$

The stable solutions will be axisymmetric droplets analogous to (5.2),

$$H(x, y; \bar{p}) \sim \tfrac{1}{4}\bar{p}(\bar{w}^2 - x^2 - y^2) \qquad 0 \le r < \bar{w}, \tag{5.13}$$

where $\bar{w}$ now gives the effective radius of the droplet. Consequently the quasi-steady form of droplets becomes

$$h(x, y, t) \sim H(x - X(\tau), y - Y(\tau); P(\tau)) + \sigma h_1. \tag{5.14}$$

Linearizing about this solution gives three solvability equations determining the motion in the plane and the evolution of the droplet pressure. These equations are now given in terms of line integrals of the flux around the perimeter of the droplet core [84, 86, 168]. Finally, extending (5.10), the flux is given in terms of the gradient of a potential, $\mathbf{J} = -\nabla V$, which satisfies Laplace's equation, $\nabla^2 V = 0$, in the precursor region (the region exterior to droplet cores), subject to Dirichlet boundary conditions $V = V(h_*(P_n))$ at the droplet perimeters.

### *5.1. Multi-scale modeling of dewetting*

Having reviewed the possible behaviors in individual coarsening events, we turn to problems of interest for systems on large physical scales which may contain very large numbers of drops, $N \gg 1$. For such large problems, accurate direct numerical simulations of the PDE are not feasible. Computations of the reduced ODE model may still be possible, but may be excessive since the particular details of how or when individual droplets coarsen out is no longer the focus. At a macro-scopic scale, what is needed is a further level of faithful reformulation of the underlying system that can efficiently capture global properties without the need for resolving the solution to full detail. This practical strategy is common to approaches for many types of complex physical systems studied using multiscale modeling [63]. For the study of dewetting films, this means that questions of

interest address how the number of remaining droplets in the system evolves, $N(t)$, what is the lengthscale between drops, $L(t)$, and further questions on the distribution of droplet sizes that can be understood from considering the set of droplets as an evolving population model.

To briefly illustrate how a statistical scaling law for the number of droplets can be obtained, we give a sketch of the heuristic argument from [87]. Assume we start with a large number of droplets on a fixed domain. The average spacing between drops will scale like $L = O(1/N)$, and since the total mass in the system is conserved for all times, the average mass similarly scales as $M = O(1/N)$. From (5.3), the typical droplet pressure will be $P = O(1/\sqrt{M}) = O(\sqrt{N})$. If we consider only collapse events and treat all other drops to be fixed while an individual droplet collapses, its pressure can be shown to obey

$$\frac{dP_n}{dt} \approx \frac{P_n^4}{L} \qquad \rightarrow \qquad P_n(t) \propto \left(\frac{L}{T_c - t}\right)^{1/3}. \tag{5.15}$$

For a droplet starting with $P = O(\sqrt{N})$, this yields an estimate on the time to collapse as $T_c = O(P^{-3}L) = O(N^{-3/2}N^{-1}) = O(N^{-5/2})$. This establishes a timescale that can be used for subsequent collapses, assuming them to be independent and uncorrelated events,

$$\frac{1}{N}\frac{dN}{dt} = -\frac{1}{T_c} \qquad \rightarrow \qquad N(t) = O(t^{-2/5}). \tag{5.16}$$

Numerical simulations of (5.11ab) show very good agreement with this scaling law. Rigorous results on upper bounds for average coarsening rates for Cahn-Hilliard equations, in terms of growth of characteristic lengthscales between localized structures, were obtained by Kohn and Otto [119]. Their analysis depends on conservation of mass in the system and estimates of the rate of dissipation of the energy. Noting that the energy (2.7) can be related to the number of drops by

$$E = \int U(h) + \tfrac{1}{2}h_x^2\, dx = O(N^{1/2}),$$

their approach was extended to provide rigorous validation for the estimate (5.16) [162].

An alternative to using global estimates from the PDE is to do further analysis of the lower-dimensional ODE model. In [47], upper bounds on coarsening rates for a model of particle growth through interaction with a dynamic mean-field was studied. That work motivated the approach in [92] to consider a simplified version of the ODE system (5.11b) restricted to collapse events only and now expressed in terms of droplet masses,

$$\frac{dM_n}{dt} = \frac{M_{n+1}^{-1/2} - M_n^{-1/2}}{L_{n+1}} - \frac{M_n^{-1/2} - M_{n-1}^{-1/2}}{L_n}, \tag{5.17}$$

where the $L_n$'s are the separation between adjacent drops and (5.3) has been used to re-write the ODE for $P_n(t)$. This system of coupled ODEs for interacting droplets can be approximated by replacing the separations with the mean separation, $L_* = L_{\text{total}}/N$, and by replacing the nearest-neighbor coupling by an effective mean-field pressure,

$$\frac{dM_n}{dt} = \frac{2}{L_*}\left(M_*^{-1/2} - M_n^{-1/2}\right) \qquad M_*^{-1/2} = \frac{1}{N}\sum_n M_n^{-1/2}, \tag{5.18}$$

where the form of $M_*$ ensures conservation of mass in this discrete system. Further analyses of this system are given in [45,46]. System (5.18) can be called a *discrete mean-field model* because while its coupling between droplets is now done in a nonlocal manner through the mean-field $M_*$, the evolution of the system still involves integrating the system of $N$ ODEs. Further, like (5.17) and (5.11b), finite-time singularities occur at each of the coarsening events and hence $N$ and $L_*$ are piecewise-defined in time between successive singularities.

A continuous mean-field model can be obtained by considering the evolution of the population of droplets as described by a distribution function $\phi = \phi(m,t)$, for the number density of drops of a given mass. In terms of this continuous distribution function, the number of droplets is given by

$$N(t) = \int_0^\infty \phi(m,t)\, dm, \tag{5.19}$$

and the mean-field pressure is the expected value of the pressure with respect to $\phi$,

$$\frac{1}{\sqrt{m_*}} = \frac{1}{N}\int_0^\infty \frac{1}{\sqrt{m}}\phi(m,t)\, dm. \tag{5.20}$$

Then a conservation law for the droplet size distribution can be written as

$$\frac{\partial \phi}{\partial t} + \frac{\partial}{\partial m}[v(m)\phi] = 0 \qquad v(m) \equiv \frac{dm}{dt} = \frac{2}{L_*}\left(\frac{1}{\sqrt{m_*}} - \frac{1}{\sqrt{m}}\right), \tag{5.21}$$

where the mass-transition rate follows from the discrete model (5.18). Equation (5.21) is a non-local conservation law since the transition rate depends on integrals of $\phi$. Following the pioneering works of Lifshitz, Slyozov, and Wagner in the 1960s [129,212] such models are called LSW equations [135]. LSW models have been the focus of extensive analysis on stability and long-time behavior of solutions [150–155]. Numerical simulations of the ODE and discrete mean field model suggest that for long times, the size droplet distribution appears to approach a self-similar form; scaling analysis of (5.21) determines this to be of the form,

$$\phi(m,t) = t^{-4/5} f(\eta), \quad \eta = mt^{-2/5}, \tag{5.22}$$

which directly yields $N(t) = O(t^{-2/5})$ from (5.19).

## 6. Open questions and directions for further work

The various stages of dewetting provide very rich problems for further study. Analysis of the dynamics in the intermediate stages may be the area of greatest need of further study as simulations and experiments have shown that many different types of patterns can develop [166]. Better understanding of the geometric aspects of instabilities in this regime may provide crucial information for describing the long-time behavior. Approaches used in studies of fluid foams [33, 193, 194] may be relevant for films forming ridge networks. While the long-time asymptotics of coarsening may follow the predictions of LSW models, it should be noted that the very long time scales involved (weeks or months in some situations) may make those limiting cases irrelevant to more typical real-world problems over seconds to minutes. Consequently, bounds on transient dynamics occurring on moderate timescales may be the results that can have greatest relevance for applications.

While dewetting is generally undesirable in many applications where uniform coatings are needed (as in painting and printing), there are important cases where dewetting can be very helpful, if it can be controlled.

One such application is the cooling of high-power electrical devices. One approach to maintain stable operating conditions in such systems, is to use heat transfer to drive phase change (evaporation/condensation) of fluids in contact with the devices [127, 177]. Engineering studies have suggested that heat transfer from solid surfaces in contact with fluids is more efficient when the fluid is in the form of sets of small drops ("dropwise condensation") rather than a single uniform film ("filmwise condensation") [127, 176]. Consequently this is a context where dewetting is very desirable. Recent experimental studies have designed strongly hydrophobic surfaces to enhance droplet formation and coarsening dynamics [8, 70, 138, 180]. One study showed that having a temperature gradient across the solid surface can dramatically change the form of the drop size distribution from that expected from LSW models for uniform temperature [134]. Other studies considered the coarsening dynamics of droplets that exchange mass through a porous substrate layer [8, 207]. Controlling the dynamics of droplet coarsening in such systems is crucial as both extremes (remaining thin precursor only or "flooded" thick film) are sub-optimal for heat transfer.

While there is a lot of research on evaporation of individual fluid droplets [36], the problem of how evaporation and condensation change the dynamics of dewetting in equations like (1.1) has received less attention [7, 34, 146, 159, 203, 215]. Such models can be written as

$$\frac{\partial h}{\partial t} = \nabla \cdot (m(h)\nabla p) - Q, \tag{6.1}$$

where $Q[h]$ is a non-conservative mass flux due to phase changes. Various forms for this flux have been used in different studies [198], but perhaps most notable is a form derived from thermodynamic conditions [3, 6] which fits in a class of forms making (6.1) a gradient flow [197–200]. Some results have been obtained for early stage dynamics [108], however the fact that fluid mass is not conserved in these models suggests that the LSW and Kohn-Otto approaches for describing the long-time coarsening dynamics will not work without novel modifications. Noting that even very weak evaporation and condensation can be expected to have cumulative influences on long-time dewetting dynamics, they could dramatically change behaviors from the mass-conserving case. In [107, 109] it was shown that $Q$ violating gradient-flow form can yield more complicated mathematical properties for (6.1) including time-periodic solutions and different forms of finite-time rupture singularities.

Microfluidics [195, 216] is another important application using surface wetting properties to manipulate small samples of fluids. Some studies have used substrates with carved channels to direct the motion of fluid droplets [99], however using flat substrates with spatially varying wetting properties can have some advantages [52, 54]. Equation (1.1) can be used to describe dynamics on a heterogeneous or "chemically patterned" substrates by including spatial dependence in the disjoining pressure, $\Pi = \Pi(h, x)$ [10, 32, 53, 98, 120, 133, 202]. Designs with hydrophilic stripes surrounded by hydrophobic regions have proved effective in confining and directing thin film flows in experiments [54]. But there are many open physical questions and need for further mathematical analysis to fully describe the dynamics and stability of such systems [5, 196]. More studies of the long-time behaviors of thin films since there is potential for different interesting behaviors to arise from the competition between coarsening (causing droplets to grow) and pinning at heterogeneous interfaces (which limits growth) [32].

We conclude by briefly noting other important directions for further related research:

- For very thin films at the scale where the disjoining pressure and molecular interactions become significant, the influences of surface roughness and thermal fluctuations may likewise be important. Several papers have examined how to derive models which include stochastic forcing and how this can affect the dynamics [55, 61, 74, 94, 137, 171].
- There has been a lot of interest in seeing how the gradient flow framework (2.7) can be extended to model and analyze more complicated physical systems with dewetting coupled to other dynamics, for example surfactants [200, 201], complex fluids [198, 199] or multi-layer flows [75, 169, 213].
- Other interesting generalizations of (1.1) in a variational framework have been obtained by including a height-dependent coefficient in the interfacial energy term in (2.7) [164, 165].
- Dewetting in flows on curved surfaces [136, 174, 178, 185] is of great interest for many physical applications and would also address questions on how large-scale spatial heterogeneities could be incorporated into mean-field models of coarsening. There are also many results for multi-dimensional problems that need different analytical approaches than in one spatial dimension and should be studied further [21, 26, 48].
- Further study is needed to see how improved models of the disjoining pressure that include curvature dependence [44, 223] modify the regularized rupture dynamics leading to dry spot formation. For non-wetting droplets on superhydrophobic substrates [138], lubrication theory can not be directly employed and dewetting dynamics may need to be derived for general Stokes flows. Other problems for merging droplets with significant inertial effects require full Navier-Stokes flows [132].
- Many of the ideas used to study finite-time rupture can also be applied to singularity formation (blow-up or pinch-off) in other higher-order PDE problems [18, 24, 25, 221] and materials science problems like solid thin films [76, 77].
- Developing better understandings of the interesting dynamics in the range of problems described above provides many challenges for both analysis and in creating efficient numerical methods that can simulate long-time dynamics of large scale systems [14, 83, 121, 222] and resolving finite-time singularities [69, 206, 218].

## Acknowledgments

The author wishes to express his appreciation to his collaborators and other colleagues in the thin films research community whose work has educated, challenged, and motivated him.

## Conflict of interest

The author declares no conflicts of interest in this paper.

## References

1. D. J. Acheson, *Elementary Fluid Dynamics*, The Clarendon Press Oxford University Press, New York, 1990.
2. V. S. Ajaev, *Evolution of dry patches in evaporating liquid films*, Phys. Rev. E, **72** (2005), 031605.

3. V. S. Ajaev, *Spreading of thin volatile liquid droplets on uniformly heated surfaces*, J. Fluid Mech., **528** (2005), 279–296.
4. V. S. Ajaev, *Interfacial Fluid Mechanics*, Springer, New York, 2012.
5. V. S. Ajaev, E. Y. Gatapova, O. A. Kabov, *Stability and break-up of thin liquid films on patterned and structured surfaces*, Adv. Colloid Interface Sci., **228** (2016), 92–104.
6. V. S. Ajaev and G. M. Homsy, *Steady vapor bubbles in rectangular microchannels*, J. Colloid Interface Sci., **240** (2001), 259–271.
7. V. S. Ajaev, J. Klentzman, T. Gambaryan-Roisman, et al. *Fingering instability of partially wetting evaporating liquids*, J. Eng. Math., **73** (2012), 31–38.
8. D. M. Anderson, M. K. Gupta, A. A. Voevodin, et al. *Using amphiphilic nanostructures to enable long-range ensemble coalescence and surface rejuvenation in dropwise condensation*, ACS Nano, **6** (2012), 3262–3268.
9. D. G. Aronson, The porous medium equation. In *Nonlinear diffusion problems (Montecatini Terme, 1985)*, volume 1224 of *Lecture Notes in Math.*, pages 1–46. Springer, Berlin, 1986.
10. M. Asgari and A. Moosavi, *Coarsening dynamics of dewetting nanodroplets on chemically patterned substrates*, Phys. Rev. E, **86** (2012), 016303.
11. G. I. Barenblatt, *Scaling, Self-similarity, and Intermediate Asymptotics*, Cambridge University Press, New York, 1996.
12. G. I. Barenblatt, *Scaling*, Cambridge University Press, New York, 2003.
13. J. Becker, G. Grün, R. Seemann, et al. *Complex dewetting scenarios captured by thin-film models*, Nat. Mater., **2** (2003), 59–63.
14. P. Beltrame and U. Thiele, *Time integration and steady-state continuation for 2d lubrication equations*, SIAM J. Appl. Dyn. Syst., **9** (2010), 484–518.
15. F. Bernis, *Finite speed of propagation and continuity of the interface for thin viscous flows*, Adv. Differential Equ., **1** (1996), 337–368.
16. F. Bernis and A. Friedman, *Higher order nonlinear degenerate parabolic equations*, J. Differ. Equations, **83** (1990), 179–206.
17. F. Bernis, J. Hulshof, J. R. King, *Dipoles and similarity solutions of the thin film equation in the half-line*, Nonlinearity, **13** (2000), 413–439.
18. A. L. Bertozzi, *Symmetric singularity formation in lubrication-type equations for interface motion*, SIAM J. Appl. Math., **56** (1996), 681–714.
19. A. L. Bertozzi, *The mathematics of moving contact lines in thin liquid films*, Notices of the American Mathematical Society, **45** (1998), 689–697.
20. A. L. Bertozzi, M. P. Brenner, T. F. Dupont, et al. Singularities and similarities in interface flows. In *Trends and perspectives in applied mathematics*, pages 155–208. Springer, New York, 1994.
21. A. L. Bertozzi, G. Grün, T. P. Witelski, *Dewetting films: bifurcations and concentrations*, Nonlinearity, **14** (2001), 1569–1592.
22. A. L. Bertozzi and M. C. Pugh, *The lubrication approximation for thin viscous films: the moving contact line with a "porous media" cut-off of van der Waals interactions*, Nonlinearity, **7** (1994), 1535–1564.
23. A. L. Bertozzi and M. C. Pugh, *The lubrication approximation for thin viscous films: regularity and long-time behavior of weak solutions*, Commun. Pure Appl. Math., **49** (1996), 85–123.

24. A. L. Bertozzi and M. C. Pugh, *Long-wave instabilities and saturation in thin film equations*, Commun. Pure Appl. Math., **51** (1998), 625–661.
25. A. L. Bertozzi and M. C. Pugh, *Finite-time blow-up of solutions of some long-wave unstable thin film equations*, Indiana Univ. Math. J., **49** (2000), 1323–1366.
26. M. Bertsch, R. Dal Passo, H. Garcke, et al. *The thin viscous flow equation in higher space dimensions*, Adv. Differ. Equations, **3** (1998), 417–440.
27. J. Bischof, D. Scherer, S. Herminghaus, et al. *Dewetting modes of thin metallic films: Nucleation of holes and spinodal dewetting*, Phys. Rev. Lett., **77** (1996), 1536–1539.
28. S. Boatto, L. P. Kadanoff, P. Olla, *Traveling-wave solutions to thin-film equations*, Phys. Rev. E, **48** (1993), 4423–4431.
29. D. Bonn, J. Eggers, J. Indekeu, et al. *Wetting and spreading*, Rev. Mod. Phys., **81** (2009), 739–805.
30. M. Bowen, J. Hulshof, J. R. King, *Anomalous exponents and dipole solutions for the thin film equation*, SIAM J. Appl. Math., **62** (2001), 149–179.
31. R. J. Braun, *Dynamics of the tear film*, Annu. Rev. Fluid Mech., **44** (2012), 267–297.
32. L. Brusch, H. Kühne, U. Thiele, et al. *Dewetting of thin films on heterogeneous substrates: Pinning versus coarsening*, Phys. Rev. E, **66** (2002), 011602.
33. L. N. Brush and S. H. Davis, *A new law of thinning in foam dynamics*, J. Fluid Mech., **534** (2005), 227–236.
34. J. P. Burelbach, S. G. Bankoff, S. H. Davis, *Nonlinear stability of evaporating/condensing liquid films*, J. Fluid Mech., **195** (1988), 463–494.
35. J. A. Carrillo and G. Toscani, *Long-time asymptotics for strong solutions of the thin film equation*, Commun. Math. Phys., **225** (2002), 551–571.
36. A.-M. Cazabat and G. Guena, *Evaporation of macroscopic sessile droplets*, Soft Matter, **6** (2010), 2591–2612.
37. S. J. Chapman, P. H. Trinh, T. P. Witelski, *Exponential asymptotics for thin film rupture*, SIAM J. Appl. Math., **73** (2013), 232–253.
38. K.-S. Chou and S.-Z. Du, *Estimates on the Hausdorff dimension of the rupture set of a thin film*, SIAM J. Math. Anal., **40** (2008), 790–823.
39. K.-S. Chou and Y.-C. Kwong, *Finite time rupture for thin films under van der Waals forces*, Nonlinearity, **20** (2007), 299–317.
40. P. Constantin, T. F. Dupont, R. E. Goldstein, et al. *Droplet breakup in a model of the Hele-Shaw cell*, Phys. Rev. E, **47** (1993), 4169–4181.
41. P. Constantin, T. Elgindi, H. Nguyen, et al. *On singularity formation in a Hele-Shaw model*, Commun. Math. Phys., **363** (2018), 139–171.
42. R. V. Craster and O. K. Matar, *Dynamics and stability of thin liquid films*, Rev. Mod. Phys., **81**(2009), 1131–1198.
43. M. C. Cross and P. C. Hohenberg, *Pattern formation outside of equilibrium*, Rev. Mod. Phys., **65** (1993), 851–1112.
44. B. Dai, L. G. Leal, A. Redondo, *Disjoining pressure for nonuniform thin films*, Phys. Rev. E, **78** (2008), 061602.

45. S. B. Dai, *On a mean field model for 1D thin film droplet coarsening*, Nonlinearity, **23** (2010), 325–340.
46. S. B. Dai, *On the Ostwald ripening of thin liquid films*, Commun. Math. Sci., **9** (2011), 143–160.
47. S. B. Dai and R. L. Pego, *Universal bounds on coarsening rates for mean-field models of phase transitions*, SIAM J. Math. Anal., **37** (2005), 347–371.
48. R. Dal Passo, H. Garcke, G. Grün, *On a fourth-order degenerate parabolic equation: global entropy estimates, existence, and qualitative behavior of solutions*, SIAM J. Math. Anal., **29** (1998), 321–342.
49. R. Dal Passo, L. Giacomelli, A. Shishkov, *The thin film equation with nonlinear diffusion*, Commun. Part. Diff. Eq., **26** (2001), 1509–1557.
50. M. C. Dallaston, M. A. Fontelos, D. Tseluiko, et al. *Discrete self-similarity in interfacial hydrodynamics and the formation of iterated structures*, Phys. Rev. Lett., **120** (2018), 34505.
51. M. C. Dallaston, D. Tseluiko, Z. Zheng, et al. *Self-similar finite-time singularity formation in degenerate parabolic equations arising in thin-film flows*, Nonlinearity, **30** (2017), 2647–2666.
52. A. A. Darhuber and S. M. Troian, *Principles of microfluidic actuation by modulation of surface stresses*, Annu. Rev. Fluid Mech., **37** (2005), 425–455.
53. A. A. Darhuber, S. M. Troian, S. M. Miller, et al. *Morphology of liquid microstructures on chemically patterned surfaces*, J. Appl. Phys., **87** (2000), 7768–7775.
54. A. A. Darhuber, S. M. Troian, W. W. Reisner, *Dynamics of capillary spreading along hydrophilic microstripes*, Phys. Rev. E, **64** (2001), 031603.
55. B. Davidovitch, E. Moro, H. A. Stone, *Spreading of viscous fluid drops on a solid substrate assisted by thermal fluctuations*, Phys. Rev. Lett., **95** (2005), 244505.
56. P. G. de Gennes, *Wetting - statics and dynamics*, Rev. Mod. Phys., **57** (1985), 827–863.
57. P. G. de Gennes, F. Brochard-Wyart, D. Quere, *Capillarity and Wetting Phenomena: Drops, Bubbles, Pearls, Waves*, Springer Verlag, New York, 2003.
58. M. di Bernardo, C. J. Budd, A. R. Champneys, et al. *Piecewise-smooth Dynamical Systems*, volume 163 of *Applied Mathematical Sciences*, Springer-Verlag London, Ltd., London, 2008.
59. J. A. Diez, A. G. Gonzalez, L. Kondic, *On the breakup of fluid rivulets*, Phys. Fluids, **21** (2009), 082105.
60. J. A. Diez and L. Kondic, *On the breakup of fluid films of finite and infinite extent*, Phys. Fluids, **19** (2007), 072107.
61. M. A. Durán-Olivencia, R. S. Gvalani, S. Kalliadasis, et al. *Instability, rupture and fluctuations in thin liquid films: Theory and computations*, J. Stat. Phys., **174** (2019), 579–604.
62. M. Dziwnik, M. Korzec, A. Münch, et al. *Stability analysis of unsteady, nonuniform base states in thin film equations*, Multiscale Model. Sim., **12** (2014), 755–780.
63. E. Weinan, *Principles of Multiscale Modeling*, Cambridge University Press, Cambridge, 2011.
64. J. Eggers, *Nonlinear dynamics and breakup of free-surface flows*, Rev. Mod. Phys., **69** (1997), 865–929.
65. J. Eggers and M. A. Fontelos, *The role of self-similarity in singularities of partial differential equations*, Nonlinearity, **22** (2009), R1–R44.
66. J. Eggers and M. A. Fontelos, *Singularities: Formation, Structure, and Propagation*, Cambridge University Press, 2015.

67. J. Eggers and L. Pismen, *Nonlocal description of evaporating drops*, Phys. Fluids, **22** (2010), 112101.
68. C. M. Elliott and H. Garcke, *On the Cahn-Hilliard equation with degenerate mobility*, SIAM J. Math. Anal., **27** (1996), 404–423.
69. S. Engelnkemper, S. V. Gurevich, H. Uecker, et al. Continuation for thin film hydrodynamics and related scalar problems. In *Computational Modelling of Bifurcations and Instabilities in Fluid Dynamics*, pages 459–501. Springer, 2019.
70. R. Enright, N. Miljkovic, J. L. Alvarado, et al. *Dropwise condensation on micro-and nanostructured surfaces*, Nanosc. Microsc. Therm., **18** (2014), 223–250.
71. P. L. Evans, J. R. King, A. Münch, *Intermediate-asymptotic structure of a dewetting rim with strong slip*, Applied Mathematics Research Express, **2006** (2006), 25262.
72. P. L. Evans, J. R. King, A. Münch, *The structure of a dewetting rim with strong slip: the long-time evolution*, Multiscale Model. Sim., **16** (2018), 1365–1391.
73. R. Fetzer, K. Jacobs, A. Munch, et al. *New slip regimes and the shape of dewetting thin liquid films*, Phys. Rev. Lett., **95** (2005), 127801.
74. J. Fischer and G. Grün, *Existence of positive solutions to stochastic thin-film equations*, SIAM J. Math. Anal., **50** (2018), 411–455.
75. L. S. Fisher and A. A. Golovin, *Nonlinear stability analysis of a two-layer thin liquid film: Dewetting and autophobic behavior*, J. Colloid Interf. Sci., **291** (2005), 515–528.
76. Y. Gao, H. Ji, J.-G. Liu, et al. *A vicinal surface model for epitaxial growth with logarithmic free energy*, Discrete & Continuous Dynamical Systems-B, **23** (2018), 4433–4453.
77. Y. Gao, J.-G. Liu, X. Y. Lu, *Gradient flow approach to an exponential thin film equation: global existence and latent singularity*, ESAIM: Control, Optimisation and Calculus of Variations, **25** (2019), 49.
78. A. Ghatak, R. Khanna, A. Sharma, *Dynamics and morphology of holes in dewetting thin films*, J. Colloid Interf. Sci., **212** (1999), 483–494.
79. L. Giacomelli, *A fourth-order degenerate parabolic equation describing thin viscous flows over an inclined plane*, Appl. Math. Lett., **12** (1999), 107–111.
80. L. Giacomelli, M. V. Gnann, F. Otto, *Regularity of source-type solutions to the thin-film equation with zero contact angle and mobility exponent between* $3/2$ *and 3*, Eur. J. Appl. Math., **24** (2013), 735–760.
81. L. Giacomelli and F. Otto, *Rigorous lubrication approximation*, Interfaces Free Bound., **5** (2003), 483–529.
82. M.-H. Giga, Y. Giga, J. Saal, *Nonlinear Partial Differential Equations: Asymptotic Behavior of Solutions and Self-Similar Solutions*, Birkhäuser Boston, Ltd., Boston, MA, 2010.
83. K. Glasner and S. Orizaga, *Improving the accuracy of convexity splitting methods for gradient flow equations*, J. Comput. Phys., **315** (2016), 52–64.
84. K. Glasner, F. Otto, T. Rump, et al. *Ostwald ripening of droplets: The role of migration*, Eur. J. Appl. Math., **20** (2009), 1–67.
85. K. B. Glasner, *Spreading of droplets under the influence of intermolecular forces*, Phys. Fluids, **15** (2003), 1837–1842.
86. K. B. Glasner, *Ostwald ripening in thin film equations*, SIAM J. Appl. Math., **6** (2008), 473–493.

87. K. B. Glasner and T. P. Witelski, *Coarsening dynamics of dewetting films*, Phys. Rev. E, **67** (2003), 016302.
88. K. B. Glasner and T. P. Witelski, *Collision versus collapse of droplets in coarsening of dewetting thin films*, Physica D, **209** (2005), 80–104.
89. M. V. Gnann and M. Petrache, *The Navier-slip thin-film equation for 3D fluid films: existence and uniqueness*, J. Differ. Equations, **265** (2018), 5832–5958.
90. R. E. Goldstein, A. I. Pesci, M. J. Shelley, *Attracting manifold for a viscous topology transition*, Phys. Rev. Lett., **75** (1995), 3665–3668.
91. C. P. Grant, *Spinodal decomposition for the Cahn-Hilliard equation*, Commun. Part. Diff. Eq., **18** (1993), 453–490.
92. M. B. Gratton and T. P. Witelski, *Transient and self-similar dynamics in thin film coarsening*, Physica D, **238** (2009), 2380–2394.
93. H. P. Greenspan, *On the motion of a small viscous droplet that wets a surface*, J. Fluid Mech., **84** (1978), 125–143.
94. G. Grün, K. Mecke, M. Rauscher, *Thin-film flow influenced by thermal noise*, J. Stat. Phys., **122** (2006), 1261–1291.
95. G. Grün and M. Rumpf, *Nonnegativity preserving convergent schemes for the thin film equation*, Numer. Math., **87** (2000), 113–152.
96. G. Grün and M. Rumpf, *Simulation of singularities and instabilities arising in thin film flow*, Eur. J. Appl. Math., **12** (2001), 293–320.
97. E. K. O. Hellen and J. Krug, *Coarsening of sand ripples in mass transfer models*, Phys. Rev. E, **66** (2002), 011304.
98. D. Herde, U. Thiele, S. Herminghaus, et al. *Driven large contact angle droplets on chemically heterogeneous substrates*, EPL, **100** (2012), 16002.
99. S. Herminghaus, M. Brinkmann, R. Seemann, *Wetting and dewetting of complex surface geometries*, Annu. Rev. Mater. Res., **38** (2008), 101–121.
100. S. Herminghaus and F. Brochard, *Dewetting though nucleation*, C. R. Phys., **7** (2006), 1073–1081.
101. S. Herminghaus, K. Jacobs, K. Mecke, et al. *Spinodal dewetting in liquid crystal and liquid metal films*, Science, **282** (1998), 916–919.
102. L. M. Hocking, *The influence of intermolecular forces on thin fluid layers*, Phys. Fluids, **5** (1993), 793–798.
103. C. Huh and L. E. Scriven, *Hydrodynamic model of steady movement of a solid/liquid/fluid contact line*, J. Colloid Interf. Sci., **35** (1971), 85–101.
104. H. J. Hwang and T. P. Witelski, *Short-time pattern formation in thin film equations*, Discrete and Continuous Dynamical Systems. Series A, **23** (2009), 867–885.
105. J. N. Israelachvili, *Intermolecular and Surface Forces*, Academic Press, New York, 1992.
106. K. Jacobs, R. Seemann, S. Herminghaus, Stability and dewetting of thin liquid films. In *Polymer thin films*, pages 243–265. World Scientific, 2008.
107. H. Ji and T. P. Witelski, *Finite-time thin film rupture driven by modified evaporative loss*, Physica D, **342** (2017), 1–15.

108. H. Ji and T. P. Witelski, *Instability and dynamics of volatile thin films*, Phys. Rev. Fluids, **3** (2018), 024001.
109. H. Ji and T. P. Witelski, *Steady states and dynamics of a thin-film-type equation with non-conserved mass*, Eur. J. Appl. Math., (2019), 1–34.
110. H. Jiang and W.-M. Ni, *On steady states of van der Waals force driven thin film equations*, Eur. J. Appl. Math., **18** (2007), 153–180.
111. S. Kalliadasis, C. Ruyer-Quil, B. Scheid, et al. *Falling Liquid Films*, volume 176 of *Applied Mathematical Sciences*, Springer, London, 2012.
112. H. S. Kheshgi and L. E. Scriven, *Dewetting - nucleation and growth of dry regions*, Chem. Eng. Sci., **46** (1991), 519–526.
113. J. R. King, *Two generalisations of the thin film equation*, Math. Comput. Model., **34** (2001), 737–756.
114. J. R. King and M. Bowen, *Moving boundary problems and non-uniqueness for the thin film equation*, Eur. J. Appl. Math., **12** (2001), 321–356.
115. J. R. King, A. Münch, B. Wagner, *Linear stability of a ridge*, Nonlinearity, **19** (2006), 2813–2831.
116. J. R. King, A. Münch, B. A. Wagner, *Linear stability analysis of a sharp-interface model for dewetting thin films*, J. Eng. Math., **63** (2009), 177–195.
117. G. Kitavtsev, L. Recke, B. Wagner, *Centre manifold reduction approach for the lubrication equation*, Nonlinearity, **24** (2011), 2347–2369.
118. G. Kitavtsev, L. Recke, B. Wagner, *Asymptotics for the spectrum of a thin film equation in a singular limit*, SIAM J. Appl. Dyn. Syst., **11** (2012), 1425–1457.
119. R. V. Kohn and F. Otto, *Upper bounds on coarsening rates*, Commun. Math. Phys., **229** (2002), 275–295.
120. R. Konnur, K. Kargupta, A. Sharma, *Instability and morphology of thin liquid films on chemically heterogeneous substrates*, Phys. Rev. Lett., **84** (2000), 931–934.
121. M.-A. Y.-H. Lam, L. J. Cummings, L. Kondic, *Computing dynamics of thin films via large scale GPU-based simulations*, Journal of Computational Physics: X, **2** (2019), 100001.
122. E. Lauga, M. P. Brenner, H. A. Stone, Microfluidics: The no-slip boundary condition. In J. Foss, C. Tropea, and A. Yarin, editors, *Handbook of Experimental Fluid Dynamics*, chapter 19, pages 1–27. Springer, 2007.
123. R. S. Laugesen and M. C. Pugh, *Linear stability of steady states for thin film and Cahn-Hilliard type equations*, Arch. Ration. Mech. An., **154** (2000), 3–51.
124. R. S. Laugesen and M. C. Pugh, *Properties of steady states for thin film equations*, Eur. J. Appl. Math., **11** (2000), 293–351.
125. R. S. Laugesen and M. C. Pugh, *Energy levels of steady states for thin-film-type equations*, J. Differ. Equations, **182** (2002), 377–415.
126. R. S. Laugesen and M. C. Pugh, *Heteroclinic orbits, mobility parameters and stability for thin film type equations*, Electron. J. Differ. Eq., **2002** (2002), 1–29.
127. R. N. Leach, F. Stevens, S. C. Langford, et al. *Dropwise condensation: Experiments and simulations of nucleation and growth of water drops in a cooling system*, Langmuir, **22** (2006), 8864–8872.

128. L. G. Leal, *Advanced Transport Phenomena: Fluid Mechanics and Convective Transport Processes*, Cambridge University Press, 2007.
129. I. M. Lifshitz and V. V. Slyozov, *The kinetics of precipitation from supersaturated solid solutions*, J. Phys. Chem. Solids, **19** (1961), 35–50.
130. R. Limary and P. F. Green, *Dewetting instabilities in thin block copolymer films: nucleation and growth*, Langmuir, **15** (1999), 5617–5622.
131. R. Limary and P. F. Green, *Dynamics of droplets on the surface of a structured fluid film: late-stage coarsening*, Langmuir, **19** (2003), 2419–2424.
132. F. Liu, G. Ghigliotti, J. J. Feng, et al. *Numerical simulations of self-propelled jumping upon drop coalescence on non-wetting surfaces*, J. Fluid Mech., **752** (2014), 39–65.
133. W. Liu and T. P. Witelski, *Steady-states of thin film droplets on chemically heterogeneous substrates*, preprint, 2020.
134. A. M. Macner, S. Daniel, P. H. Steen, *Condensation on surface energy gradient shifts drop size distribution toward small drops*, Langmuir, **30** (2014), 1788–1798.
135. J. A. Marqusee and J. Ross, *Kinetics of phase transitions: Theory of Ostwald ripening*, J. Chem. Phys., **79** (1983), 373–378.
136. L. C. Mayo, S. W. McCue, T. J. Moroney, et al. *Simulating droplet motion on virtual leaf surfaces*, Roy. Soc. Open Sci., **2** (2015), 140528.
137. K. Mecke and M. Rauscher, *On thermal fluctuations in thin film flow*, Journal of Physics: Condensed Matter, **17** (2005), S3515.
138. N. Miljkovic, R. Enright, E. N. Wang, *Effect of droplet morphology on growth dynamics and heat transfer during condensation on superhydrophobic nanostructured surfaces*, ACS Nano, **6** (2012), 1776–1785.
139. A. Miranville, *The Cahn–Hilliard equation and some of its variants*, AIMS Mathematics, **2** (2017), 479–544.
140. V. Mitlin, *Dewetting revisited: New asymptotics of the film stability diagram and the metastable regime of nucleation and growth of dry zones*, J. Colloid Interf. Sci., **227** (2000), 371–379.
141. V. S. Mitlin, *Dewetting of a solid surface: analogy with spinodal decomposition*, J. Colloid Interf. Sci., **156** (1993), 491–497.
142. V. S. Mitlin and N. V. Petviashvili, *Nonlinear dynamics of dewetting: kinetically stable structures*, Phys. Lett. A, **192** (1994), 323–326.
143. R. Mukherjee and A. Sharma, *Instability, self-organization and pattern formation in thin soft films*, Soft matter, **11** (2015), 8717–8740.
144. A. Münch and B. Wagner, *Contact-line instability of dewetting thin films*, Physica D, **209** (2005), 178–190.
145. A. Münch, B. Wagner, T. P. Witelski, *Lubrication models with small to large slip lengths*, J. Eng. Math., **53** (2005), 359–383.
146. N. Murisic and L. Kondic, *On evaporation of sessile drops with moving contact lines*, J. Fluid Mech., **679** (2011), 219–246.
147. T. G. Myers, *Thin films with high surface tension*, SIAM Review, **40** (1998), 441–462.
148. C. Neto, K. Jacobs, R. Seemann, et al. *Correlated dewetting patterns in thin polystyrene films*, Journal of Physics: Condensed Matter, **15** (2003), S421–S426.

149. C. Neto, K. Jacobs, R. Seemann, et al. *Satellite hole formation during dewetting: experiment and simulation*, Journal of Physics: Condensed Matter, **15** (2003), 3355–3366.
150. B. Niethammer, *Derivation of the LSW-theory for Ostwald ripening by homogenization methods*, Arch. Ration. Mech. An., **147** (1999), 119–178.
151. B. Niethammer, The mathematics of Ostwald ripening. In *Geometric analysis and nonlinear partial differential equations*, pages 649–663. Springer, Berlin, 2003.
152. B. Niethammer and R. L. Pego, *Non-self-similar behavior in the LSW theory of Ostwald ripening*, J. Stat. Phys., **95** (1999), 867–902.
153. B. Niethammer and R. L. Pego, *On the initial-value problem in the Lifshitz-Slyozov-Wagner theory of Ostwald ripening*, SIAM J. Math. Anal., **31** (2000), 467–485.
154. B. Niethammer and R. L. Pego, *Well-posedness for measure transport in a family of nonlocal domain coarsening models*, Indiana U. Math. J., **54** (2005), 499–530.
155. B. Niethammer and J. J. L. Velázquez, *On the convergence to the smooth self-similar solution in the LSW model*, Indiana U. Math. J., **55** (2006), 761–794.
156. A. Novick-Cohen, The Cahn-Hilliard equation. In *Handbook of differential equations: evolutionary equations. Vol. IV*, Handb. Differ. Equ., pages 201–228. Elsevier/North-Holland, Amsterdam, 2008.
157. A. Novick-Cohen and L. A. Segel, *Nonlinear aspects of the Cahn-Hilliard equation*, Physica D, **10** (1984), 277–298.
158. J. R. Ockendon and H. Ockendon, *Viscous Flow*, Cambridge University, Cambridge, 1995.
159. A. Oron and S. G. Bankoff, *Dewetting of a heated surface by an evaporating liquid film under conjoining/disjoining pressures*, J. Colloid Interf. Sci., **218** (1999), 152–166.
160. A. Oron and S. G. Bankoff, *Dynamics of a condensing liquid film under conjoining/disjoining pressures*, Phys. Fluids, **13** (2001), 1107–1117.
161. A. Oron, S. H. Davis, S. G. Bankoff, *Long-scale evolution of thin liquid films*, Rev. Mod. Phys., **69** (1997), 931–980.
162. F. Otto, T. Rump, D. Slepcev, *Coarsening rates for a droplet model: rigorous upper bounds*, SIAM J. Math. Anal., **38** (2006), 503–529.
163. S. B. G. O'Brien and L. W. Schwartz, Theory and Modeling of Thin Film Flows, In *Encyclopedia of Surface and Colloid Science*, pages 5283–5297. Marcel Dekker, 2002.
164. A. A. Pahlavan, L. Cueto-Felgueroso, A. E. Hosoi, et al. *Thin films in partial wetting: Stability, dewetting and coarsening*, J. Fluid Mech., **845** (2018), 642–681.
165. A. A. Pahlavan, L. Cueto-Felgueroso, G. H. McKinley, et al. *Thin films in partial wetting: internal selection of contact-line dynamics*, Phys. Rev. Lett., **115** (2015), 034502.
166. D. Peschka, S. Haefner, L. Marquant, et al. *Signatures of slip in dewetting polymer films*, P. Natl. Acad. Sci. USA, **116** (2019), 9275–9284.
167. L. M. Pismen, *Spinodal dewetting in a volatile liquid film*, Phys. Rev. E, **70** (2004), 021601.
168. L. M. Pismen and Y. Pomeau, *Mobility and interactions of weakly nonwetting droplets*, Phys. Fluids, **16** (2004), 2604–2612.
169. A. Pototsky, M. Bestehorn, D. Merkt, et al. *Alternative pathways of dewetting for a thin liquid two-layer film*, Phys. Rev. E, **70** (2004), 025201.

170. C. Pozrikidis, *Boundary Integral and Singularity Methods for Linearized Viscous Flow*, Cambridge Texts in Applied Mathematics. Cambridge University Press, Cambridge, 1992.
171. M. Rauscher and S. Dietrich, *Wetting phenomena in nanofluidics*, Annu. Rev. Mater. Res., **38** (2008), 143–172.
172. G. Reiter, *Dewetting of thin polymer films*, Phys. Rev. Lett., **68** (1992), 75–78.
173. S. N. Reznik and A. L. Yarin, *Spreading of a viscous drop due to gravity and capillarity on a horizontal or an inclined dry wall*, Phys. Fluids, **14** (2002), 118–132.
174. A. J. Roberts and Z. Li, *An accurate and comprehensive model of thin fluid flows with inertia on curved substrates*, J. Fluid Mech., **553** (2006), 33–73.
175. N. O. Rojas, M. Argentina, E. Cerda, et al. *Inertial lubrication theory*, Phys. Rev. Lett., **104** (2010), 187801.
176. J. W. Rose, *On the mechanism of dropwise condensation*, Int. J. Heat Mass Tran., **10** (1967), 755–762.
177. J. W. Rose, *Dropwise condensation theory and experiment: A review*, Journal of Power Energy, **216** (2012), 115–128.
178. R. V. Roy, A. J. Roberts, M. E. Simpson, *A lubrication model of coating flows over a curved substrate in space*, J. Fluid Mech., **454** (2002), 235–261.
179. E. Ruckenstein and R. K. Jain, *Spontaneous rupture of thin liquid films*, Journal of the Chemical Society-Faraday Transactions II, **70** (1974), 132–147.
180. K. Rykaczewski, A. T. Paxson, M. Staymates, et al. *Dropwise condensation of low surface tension fluids on omniphobic surfaces*, Scientific reports, **4** (2015), 4158.
181. E. Sander and T. Wanner, *Monte Carlo simulations for spinodal decomposition*, J. Stat. Phys., **95** (1999), 925–948.
182. E. Sander and T. Wanner, *Unexpectedly linear behavior for the Cahn-Hilliard equation*, SIAM J. Appl. Math., **60** (2000), 2182–2202.
183. L. W. Schwartz, Unsteady simulation of viscous thin-layer flows. In P. A. Tyvand, editor, *Free surface flows with viscosity*, pages 203–233. Computational Mechanics Publications, Boston, 1997.
184. L. W. Schwartz, R. V. Roy, R. R. Eley, et al. *Dewetting patterns in a drying liquid film*, J. Colloid Interf. Sci., **234** (2001), 363–374.
185. L. W. Schwartz and D. E. Weidner, *Modeling of coating flows on curved surfaces*, J. Eng. Math., **29** (1995), 91–103.
186. R. Seemann, S. Herminghaus, K. Jacobs, *Dewetting patterns and molecular forces: a reconciliation*, Phys. Rev. Lett., **86** (2001), 5534–5537.
187. A. Sharma, *Many paths to dewetting of thin films*, Eur. Phys. J. E, **12** (2003), 397–407.
188. A. Sharma and R. Khanna, *Pattern formation in unstable thin liquid films*, Phys. Rev. Lett., **81** (1998), 3463–3466.
189. A. Sharma and G. Reiter, *Instability of thin polymer films on coated substrates: rupture, dewetting, and drop formation*, J. Colloid Interf. Sci., **178** (1996), 383–399.
190. A. Sharma and R. Verma, *Pattern formation and dewetting in thin films of liquids showing complete macroscale wetting: From "pancakes" to "swiss cheese"*, Langmuir, **20** (2004), 10337–10345.

191. D. N. Sibley, A. Nold, N. Savva, et al. *A comparison of slip, disjoining pressure, and interface formation models for contact line motion through asymptotic analysis of thin two-dimensional droplet spreading*, J. Eng. Math., **94** (2015), 19–41.
192. V. M. Starov, M. G. Velarde, C. J. Radke, *Wetting and Spreading Dynamics*, CRC Press, Boca Raton Florida, 2007.
193. P. S. Stewart and S. H. Davis, *Dynamics and stability of metallic foams: Network modeling*, J. Rheol., **56** (2012), 543–574.
194. P. S. Stewart and S. H. Davis, *Self-similar coalescence of clean foams*, J. Fluid Mech., **722** (2013), 645–664.
195. H. A. Stone, A. D. Stroock, A. Ajdari, *Engineering flows in small devices: microfluidics toward a lab-on-a-chip*, Annu. Rev. Fluid Mech., **36** (2004), 381–411.
196. U. Thiele, *Open questions and promising new fields in dewetting*, Eur. Phys. J. E, **12** (2003), 409–414.
197. U. Thiele, *Thin film evolution equations from (evaporating) dewetting liquid layers to epitaxial growth*, Journal of Physics: Condensed Matter, **22** (2010), 084019.
198. U. Thiele, *Patterned deposition at moving contact lines*, Adv. Colloid Interfac., **206** (2014), 399–413.
199. U. Thiele, *Recent advances in and future challenges for mesoscopic hydrodynamic modelling of complex wetting*, Colloids and Surfaces A, **553** (2018), 487–495.
200. U. Thiele, A. J. Archer, L. M. Pismen, *Gradient dynamics models for liquid films with soluble surfactant*, Phys. Rev. Fluids, **1** (2016), 083903.
201. U. Thiele, A. J. Archer, M. Plapp, *Thermodynamically consistent description of the hydrodynamics of free surfaces covered by insoluble surfactants of high concentration*, Phys. Fluids, **24** (2012), 102107.
202. U. Thiele and E. Knobloch, *Driven drops on heterogeneous substrates: Onset of sliding motion*, Phys. Rev. Lett., **97** (2006), 204501.
203. U. Thiele, M. Mertig, W. Pompe, *Dewetting of an evaporating thin liquid film: Heterogeneous nucleation and surface instability*, Phys. Rev. Lett., **80** (1998), 2869–2872.
204. U. Thiele, M. G. Velarde, K. Neuffer, et al. *Film rupture in the diffuse interface model coupled to hydrodynamics*, Phys. Rev. E, **64** (2001), 031602.
205. D. Tseluiko and D. T. Papageorgiou, *Nonlinear dynamics of electrified thin liquid films*, SIAM J. Appl. Math., **67** (2007), 1310–1329.
206. D. Tseluiko, J. Baxter, U. Thiele, *A homotopy continuation approach for analysing finite-time singularities in thin liquid films*, IMA J. Appl. Math., **78** (2013), 762–776.
207. H. B. van Lengerich, M. J. Vogel, P. H. Steen, *Coarsening of capillary drops coupled by conduit networks*, Phys. Rev. E, **82** (2010), 66312.
208. F. Vandenbrouck, M. P. Valignat, A. M. Cazabat, *Thin nematic films: metastability and spinodal dewetting*, Phys. Rev. Lett., **82** (1999), 2693–2696.
209. S. J. VanHook, M. F. Schatz, W. D. McCormick, et al. *Long-wavelength surface-tension-driven Bénard convection: experiment and theory*, J. Fluid Mech., **345** (1997), 45–78.
210. J. L. Vázquez, *The Porous Medium Equation*, Oxford Mathematical Monographs. The Clarendon Press, Oxford University Press, Oxford, 2007.

211. A. Vrij, *Possible mechanism for spontaneous rupture of thin free liquid films*, Discussions of the Faraday Society, **42** (1966), 23–33.
212. C. Wagner, *Theorie der alterung von niedershlagen durch umlosen (Ostwald-Reifung)*, Z. Elektrochem, **65** (1961), 581–591.
213. M. H. Ward, *Interfacial thin films rupture and self-similarity*, Phys. Fluids, **23** (2011), 062105.
214. S. J. Watson, F. Otto, B. Y. Rubinstein, et al. *Coarsening dynamics of the convective Cahn-Hilliard equation*, Physica D, **178** (2003), 127–148.
215. T. Wei and F. Duan, *Interfacial stability and self-similar rupture of evaporating liquid layers under vapor recoil*, Phys. Fluids, **28** (2016), 124106.
216. G. M. Whitesides, *The origins and the future of microfluidics*, Nature, **442** (2006), 368–373.
217. M. B. Williams and S. H. Davis, *Nonlinear theory of film rupture*, J. Colloid Interf. Sci., **90** (1982), 220–228.
218. T. P. Witelski, Computing finite-time singularities in interfacial flows. In G. Sabidussi, editor, *Modern Methods in Scientific Computing and Applications*, NATO ASI series proceedings, pages 451–487. Kluwer, 2002.
219. T. P. Witelski and A. J. Bernoff, *Stability of self-similar solutions for van der Waals driven thin film rupture*, Phys. Fluids, **11** (1999), 2443–2445.
220. T. P. Witelski and A. J. Bernoff, *Dynamics of three-dimensional thin film rupture*, Physica D, **147** (2000), 155–176.
221. T. P. Witelski, A. J. Bernoff, A. L. Bertozzi, *Blowup and dissipation in a critical-case unstable thin film equation*, Eur. J. Appl. Math., **15** (2004), 223–256.
222. T. P. Witelski and M. Bowen, *ADI schemes for higher-order nonlinear diffusion equations*, Appl. Numer. Math., **45** (2003), 331–351.
223. Q. Wu and H. Wong, *A slope-dependent disjoining pressure for non-zero contact angles*, J. Fluid Mech., **506** (2004), 157–185.
224. W. W. Zhang and J. R. Lister, *Similarity solutions for van der Waals rupture of a thin film on a solid substrate*, Phys. Fluids, **11** (1999), 2454–2462.
225. L. Zhornitskaya and A. L. Bertozzi, *Positivity-preserving numerical schemes for lubrication-type equations*, SIAM J. Numer. Anal., **37** (2000), 523–555.


AIMS Press

© 2020 the Author(s), licensee AIMS Press. This is an open access article distributed under the terms of the Creative Commons Attribution License (http://creativecommons.org/licenses/by/4.0)